Food Chemistry 140 (2013) 700–710

Contents lists available at SciVerse ScienceDirect

Food Chemistry

journal homepage: www.elsevier.com/locate/foodchem

Biosensors for monitoring the isothermal breakdown kinetics of peanut oil heated at 180 °C. Comparison with results obtained for extra virgin olive oil

M. Tomassetti [a,*], S. Vecchio [b], L. Campanella [a], R. Dragone [c]

[a] Department of Chemistry, University of Rome "La Sapienza", P.le Aldo Moro 5, I-00185 Rome, Italy
[b] Department SBAI, University of Rome "La Sapienza", via del Castro Laurenziano 7, I-00161 Rome, Italy
[c] Institute of Nanostructured Materials – CNR, c/o Department of Chemistry, Rome University "La Sapienza", P.le Aldo Moro 5, I-00185 Rome, Italy

ARTICLE INFO

Article history:
Available online 10 November 2012

Keywords:
Peanut oil
Olive oil
Thermal oxidation
Kinetic constant

ABSTRACT

The present research was devoted to studying the kinetics of the artificial rancidification of peanut oil (PO) when a sample of this oil was isothermally heated at 180 °C in an air stream. The formation of radical species due to heating was evaluated using a radical index whose value was determined using a biosensor method based on a superoxide dismutase (SOD), while the increasing toxicity was monitored using a suitable toxicity measuring probe based on the Clark electrode and immobilized yeast cells.

An extra virgin olive oil was isothermally rancidified under the same experimental conditions and the corresponding data were used for the purpose of comparison.

Both the so-called "model-fitting" and the classical kinetic methods were applied to the isothermal process biosensor data in order to obtain the kinetic constant rate value at 180 °C.

1. Introduction

In recent years, in-depth research was carried out in our laboratory on the isothermal rancidification of extra-virgin olive oil (EVOO) performed at 98 °C (Tomassetti, Vecchio, & Campanella, 2011) in an air stream, using the classical A.O.M. method (AOCS, 1964). The kinetic rate of this process was also computed. A thermal decomposition study of monovarietal EVOO samples was also performed and a relation between the kinetic parameter of decomposition and the chemical composition of the samples was established (Vecchio, Cerretani, Bendini, & Chiavaro, 2009).

The aim of the present research was instead to study the kinetic rancidification of peanut oil (PO) when a sample of this oil was artificially rancidified isothermally at 180 °C in air; in practice the oil sample was heated to a high temperature, in order to determine the constant rate value and therefore the time span over which the product can effectively and safely be used for cooking and frying. However, as reported in literature (Buzás, Simon, & Holló, 1979; Campanella, Dragone, Fisco, & Tomassetti, 2004; Lorusso & Zelinotti, 1985; Tan & Che Man, 2000), the process of heating the oil samples (Carrasco-Pancorbo et al., 2007; Chiavaro et al., 2007; Kiritsakis & Markakis, 1987; Vazquez Roncero, Janer Del Valle, & Janer Del Valle, 1973) leads to chemical changes and causes the formation of radical species, which results in an appreciable increase in oil toxicity. In the present study, radical species formation due to heating was evaluated using a radical index. This was detected using a biosensor method (Amati et al., 2008; Campanella, De Luca, Favero, Persi, & Tomassetti, 2001a) based on a superoxide dismutase (SOD) obtained by coupling an amperometric Clark-type electrode with immobilised SOD enzyme operating in dimethylsulphoxide (DMSO), while the increasing toxicity was monitored using a suitable toxicity measuring probe (Campanella et al., 2004) consisting of an oxygen sensor + yeast immobilised cells.

Two different kinetic methods for processing data derived from biosensor measurements exploited during the isothermal breakdown of peanut oil at 180 °C were used. The corresponding data for a dephenolized extra-virgin olive oil were used for the purpose of comparison. Lastly, to complete the information regarding the principal decomposition processes affecting the triglycerides during the heating of the two food oils tested, the latter were subjected to thermal analysis: thermogravimetry (TG) and first-order derivative thermogravimetry (DTG). The data obtained, processed according to the Kissinger method (Vecchio, Campanella, Nuccilli, & Tomassetti, 2008), enabled the activation energy of the thermoxidation processes occurring in the triglycerides present to be assessed.

2. Materials and methods

2.1. Chemicals

Superoxide dismutase (SOD) (EC 1.15.1.1) from bovine erythrocytes, 7000 Units mg^{-1}, dimethyl sulphoxide (DMSO), potassium

* Corresponding author. Tel.: +39 0649913722; fax: +39 06490631.
E-mail address: mauro.tomassetti@uniroma1.it (M. Tomassetti).

0308-8146/$ - see front matter © 2012 Elsevier Ltd. All rights reserved.
http://dx.doi.org/10.1016/j.foodchem.2012.10.131

superoxide, silicon oil 350 Cps Crual srl, the internal solution of the Clark electrode, namely phosphate buffer solution 0.067 mol L^{-1}, pH = 7.5, were supplied by Sigma–Aldrich. Kappa-carrageenan was supplied by Fluka, while Yellow Springs supplied the gas PTFE permeable membrane (YSI model 5775). Monobasic and dibasic potassium phosphates RPE were supplied by Carlo Erba Reagents; potassium chloride was supplied by Riedel-de Haën (Seelze, Germany).

The cells used belonged to a *Saccharomyces cerevisiae*, wild-type W303-1a diploid strain, kindly made available by the Rome Botanical Gardens. The following reagents were used for the culture medium: yeast extract for microbiology, universal peptone for microbiology M66, D-glucose for microbiology, all of analytical grade, and high purity agar agar were all supplied by Merck, Darmstadt (Germany). The dialysis membrane (art. D-9777) was supplied by Sigma, St. Louis, MO (USA); Hepes buffer, was supplied by Fluka AG, Buchs (Switzerland).

2.2. Samples

Both the commercial peanut and extra-virgin olive oil samples analyzed (denoted as PO and EVOO, respectively), stored in sealed dark glass bottles, were purchased from a local shop and are marketed by a single supplier operating in Central Italy.

As the polyphenolic compounds contained in the EVOO can react with the superoxide radicals, which are introduced into the measurement solution as described in the SOD biosensor method for the radical determination, a decrease in the superoxide radical concentration in solution occurs, thus interfering with the correct application of the method (Amati et al., 2008). The EVOO samples were therefore subjected to the same isothermal rancidification process that occurred at 180 °C as well as PO samples, but only after being previously pretreated with active carbon in order to remove practically all of the polyphenolic compounds and other antioxidants contained in the EVOO (Campanella, Favero, Pastorino, & Tomassetti, 1999). Indeed all the measurements carried out in the present research regarding the EVOO samples were performed after treating the oil with active carbon, while all the measurements in PO were performed in the oil as such, because of the absence of polyphenols in this kind of oil.

2.3. Apparatus

The oxidative thermal degradation of PO and EVOO samples examined in this study took place in a silicon oil-based thermostatic bath (at 180 °C ± 0.1) in an air stream of 140 mL min^{-1} generated by a Unistar mod. AIR 1000–1 pump.

The transducer employed for the evaluation of free radicals in the oil sample using the SOD biosensor and to monitor oil sample toxicity was an Orion model 97-08-99 electrode able to measure O_2 concentration and connected to an Orion pH-meter SA720 and an Amel model 868 recorder.

All the SOD-sensor tests were carried out at 23 °C, while the toxicity tests were performed at 25 °C in a thermostatted glass cell equipped with a forced water circulation jacket coupled to a model VC 20B Julabo (Germany) thermostat. The solvents used in the tests were kept under slight but constant magnetic stirring using a microstirrer from Velp Scientifica (Italy).

The TG–DTG measurements were carried out at different heating rates (from 5 to 12.5 °C min^{-1}) using TG 50 Mettler TG equipment with a TC10-TA processor.

All thermogravimetric runs were performed on a 7–12 mg of sample, from room temperature up to about 550 °C under a 100 cm^3 min^{-1} air stream.

2.4. Methods

2.4.1. Artificial rancidification process

The artificial oxidation of an oil sample was obtained by placing the sample in a pyrex glass tube (containing 25 mL of sample under a constant stream of air of 140 mL min^{-1} according to the A.O.M. method (AOCS, 1964), while the tube was immersed in a silicon oil thermostatic bath at 180 °C, instead of at 98 °C, as required by the latter method (AOCS, 1964).

The apparatus used (see Fig. 1) had previously been illustrated in detail (Amati et al., 2008; Campanella et al., 1999). During the artificial rancidification process under isothermal conditions at the selected temperature fixed amounts of the sample contained in the glass test tube were collected at regular time intervals and immediately analyzed.

2.4.2. Superoxide dismutase (SOD) biosensor for radical determination

The concentration of free radicals was determined using an enzymatic SOD biosensor respectively applied both to the crude oil analysis of sample and to all the oil samples tested during thermal degradation.

For this analysis a superoxide dismutase biosensor operating in dimethylsulphoxide described in detail in a previous paper (Campanella et al., 2001a) was used. This biosensor was prepared by sandwiching a kappa-carrageenan gel disk (0.5 cm diameter) on which the SOD enzyme was adsorbed (Campanella et al., 2001a) between an external PTFE membrane and an internal 0.1 cm thick membrane of cellulose acetate, both fixed to the Clark electrode by a PTFE O-ring. It is important to stress that the membrane separating the organic solvent from the gel disk was made of PTFE in order to prevent the organic solvent from spreading over the kappa-carrageenan disk in which the enzyme was immobilized and denaturing the latter. The experiments were performed in a thermostatted cell at 23 °C under continuous magnetic stirring (200 rpm). As already extensively reported in literature (Campanella, Sammartino, Tomassetti, & Zannella, 2001b; Campanella et al., 2004; Kiritsakis & Markakis, 1987), heating of oil samples determines chemical changes leading to the formation of different compounds (Biffoli, 1984, chaps. 9–10); among the latter, the radical species are those

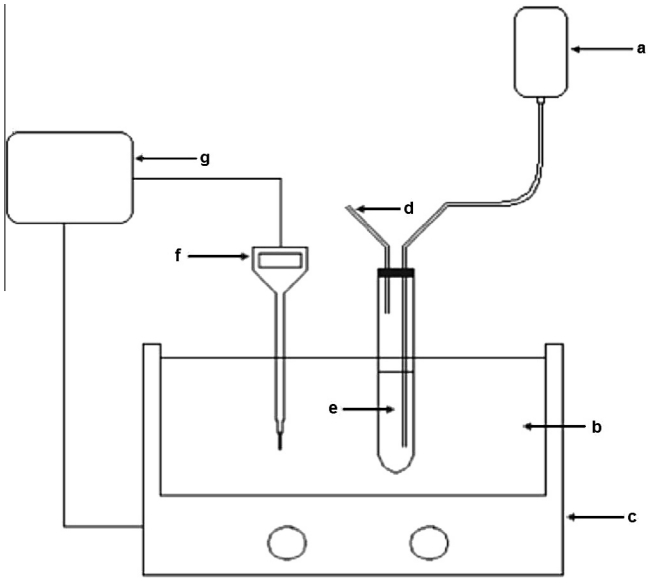

Fig. 1. Scheme of the apparatus used to study the isothermal degradation of EVOO at 180 °C under an oxidized atmosphere. (a) Air pump; (b) silicon oil bath (SOB) heated at 180 °C; (c) heating unit for the temperature of SOB; (d) breather pipe; (e) EVOO sample in *pyrex* tube with teflon cap; (f) Vertex-thermometer; (g) feeder.

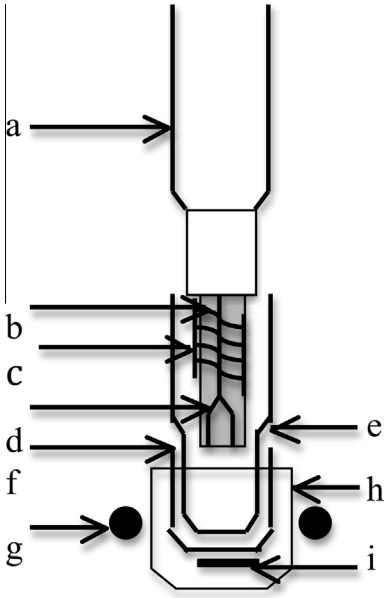

Fig. 2. SOD biosensor assembly (working in non aqueous solution) using an amperometric gas diffusion oxygen electrode as transducer with one external gas permeable membrane. The solvent used was DMSO. In the case of the EVOO this process was performed in the previously dephenolized oil. (a) Clark electrode body; (b) dielectric; (c) Ag/AgCl anode; (d) Pt cathode; (e) electrode teflon cap filled with internal solution; (f) cellulose acetate membrane; (g) teflon O-ring; (h) gas permeable membrane; (i) superoxide dismutase enzyme immobilised in kappa-carrageenan gel; (l) filling solution (phosphate buffer 0.067 mol l^{-1}, KCl 0.1 mol l^{-1}, pH 6.6).

that especially cause an appreciable increase in oil toxicity. In this study, the presence of these species in the overheated oil, which was subjected to a forced rancidification process, was detected using an indirect method based on a SOD biosensor obtained by coupling an amperometric Clark-type electrode to the immobilized SOD enzyme (Fig. 2). The electrode used was built entirely of PTFE and appropriately assembled so as to be able to operate in dimethylsulphoxide (DMSO) instead of in aqueous solution in which the oily sample is practically insoluble. SOD is an enzyme that catalyzes the following reaction:

$$O_2^{\cdot-} + O_2^{\cdot-} + 2H^+ \xrightarrow{SOD} O_2 + H_2O_2$$

As a result, when the superoxide anion was present in solution, the Clark electrode, which acts as the biosensor transducer, measured the increase in O_2 concentration caused by the enzymatic reaction due to the immobilized SOD enzyme. The method consisted in adding a PO sample (or a previously dephenolized EVOO sample) after heating under isothermal conditions for a set time at 180 °C to a DMSO solution containing the superoxide anion. In order to obtain the superoxide radical in solution, a DMSO solution of KO_2 was prepared in which the radical was quickly produced. After adding this solution to the DMSO the signal increase was recorded until a second steady state was reached as the enzyme catalyzed the superoxide radical into oxygen and hydrogen peroxide. When the oil sample containing the radical species formed during the heating process was added, this steady state was perturbed by the reactions of the radicals contained in the rancid oil with the superoxide radical previously generated in solution. As a consequence, the concentration of the superoxide radical in solution decreased and the O_2 concentration – the product of the reaction catalyzed by the SOD enzyme in solution – thus also decreased. This decrease was linked to the concentration of radicals in the heated oil. The ratio between the changes in O_2 concentration detected respectively before (a) and after (b) the addition of the oil

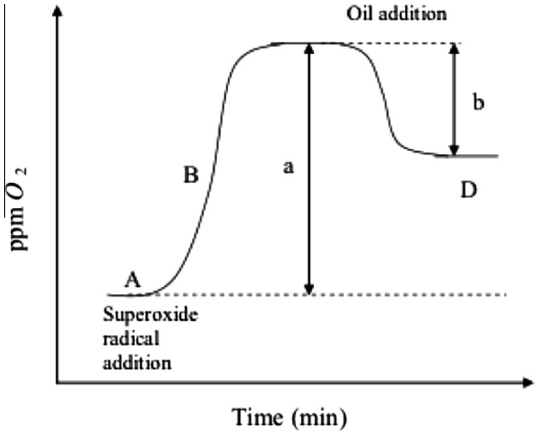

Fig. 3. Trend of the experimental curve for the determination of the free radical index *b*/*a*.

sample is linked to the concentration of the radicals formed in the oil. This ratio, *b*/*a*, provides an index of the radical formation.

In practice, in a 40 mL glass cell containing 15 mL of dimethylsulphoxide the biosensor was introduced and immersed at a depth that was maintained rigorously constant in all tests. After the signal had stabilized for about 10 min at an O_2 value of 8.4 ppm, 100 μL of a 0.03 mol L^{-1} superoxide radical in a dimethylsulphoxide solution was added. In this solution the superoxide radical was obtained by the following reaction: $KO_2 \rightarrow K^+ + O_2^{\cdot-}$

After passing through the PTFE membrane (Campanella et al., 2001a) the superoxide radicals were readily decomposed by the SOD enzyme catalyst to produce O_2, which was detected by the sensor. After a stationary state was reached and the signal variation read off, (a) 100 μL of oil were added and the corresponding decrease in the signal was recorded until a new steady state was reached (b). The measurement of the current variations corresponding to the three stationary states of the curve was used to determine the value of the *b*/*a* index, which is proportional to the amount of radicals contained in the oil samples subjected to the rancidification process (see Fig. 3).

2.4.3. Respirometric measurements to monitor oil sample toxicity

The respirometric measurements to monitor the total sample toxicity were carried out using a suitable toxicity measuring probe consisting of a Clark type oxygen sensor coupled to yeast immobilized cells.

2.4.4. Cells growth and immobilisation in agarised culture medium

The composition of the medium used to develop *Saccharomyces cerevisiae* cells was as follows: yeast extract 1%, peptone 1% and glucose 2%; of course, in the case of agar cell cultures, 1% by weight of agar was also added. The cells were immobilised on agar gel containing the culture medium (agarised medium) in the form of a layer on a sterile Petri dish, obtained by pouring 10 mL of previously sterilized 'agarised medium' in the liquid state on to the dish, allowing it to gel, and then closing and sealing the dish and storing it in a refrigerator. The yeast cells were immobilised as follows: a sterile Petri dish containing 'agarised medium' in gel form was inoculated with 200 μL *Saccharomyces cerevisiae* cell suspension obtained by allowing cells to grow for 30 h at 37 °C under stirring in a 100 mL Erlenmeyer flask containing 50 mL of culture medium. The cells were then scattered over the entire surface of the 'agarised medium' layer on the dish using a curved glass rod and allowed to grow for 48 h at room temperature. This produced a cell culture 'carpet' in which the cell colonies were entrapped and scattered fairly uniformly over the entire surface of the dish.

2.4.5. Biosensor assembly

A suitably sized disk (about 8 mm in diameter and about 1 mm thick) was thus cut out of the 'agarised medium' stratified on the Petri dish and containing the entrapped yeast cells. This disk was removed from the dish and placed between a dialysis membrane, or a nylon net and the gas permeable membrane of the Clark electrode, the whole assembly being secured to the head of the electrode by means of an O-ring. The complete system is illustrated in Fig. 4.

The biosensor is immersed in the solution contained in the thermostatted measurement cell under constant magnetic stirring. The electrode response was expressed directly in ppm O_2, by the Orion Microprocessor ionalyzer to which it was connected and could be simultaneously observed on the Amel analog recorder as a function of time.

2.4.6. Principle of the method

The yeast *Saccharomyces cerevisiae* is an important biological indicator as it is a eukaryotic single-cell organism, structurally and functionally akin to an animal cell and thus used as a 'model' in many biological studies (Kurtz, Dufour, Duclos, Bergerat, & Exinger, 2004).

The purpose of this measurement was therefore to assess any biological damage to the yeast cells caused by toxic compounds formed due to alteration of the oil in the heating process. Biological damage was assessed by monitoring the inhibition of cellular respiratory activity. This was done by immersing the Clark electrode with immobilized yeast cells over its head in an isotonic aqueous solution (≈0.3 osmomol). After a stationary state was reached by the dissolved oxygen concentration in the solution at the working temperature, a fixed volume of standard glucose solution was then added. After addition, a rapid decrease in oxygen was observed due to the respiration of the yeast cells. The decrease in oxygen concentration in the solution displayed an almost linearly decreasing trend as a function of time until it reached a new stationary state. In practice, this new stationary state was attained

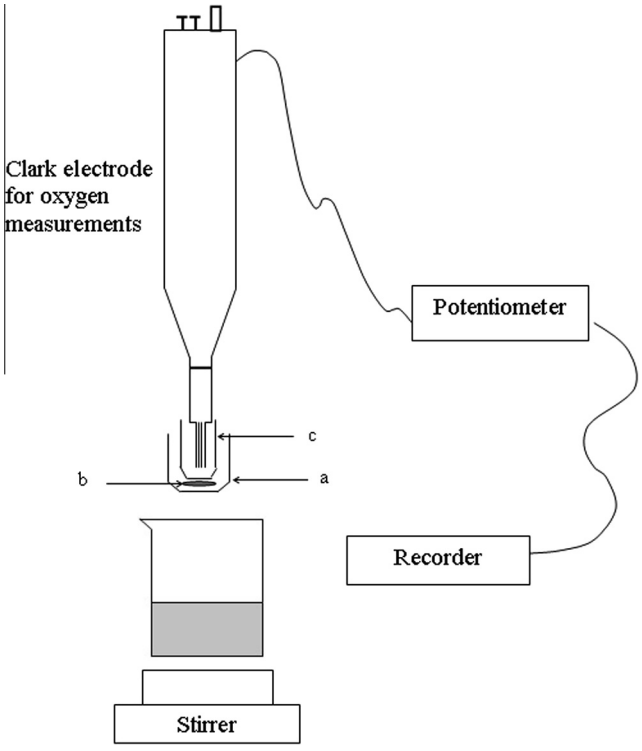

Fig. 4. Probe for measurement of oil toxicity: (a) nylon net; (b) yeast cells entrapped in agarised medium; (c) dialysis membrane.

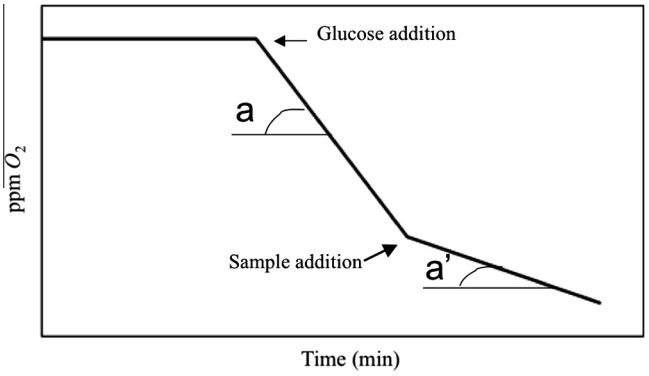

Fig. 5. Scheme of the experimental respirometric curve for the determination of a'/a value linked to the inhibition respirometric index "ρ".

when the rate at which atmospheric oxygen permeated the solution and the rate at which dissolved oxygen was consumed in cellular respiration were the same. If the test sample, that is an oil previously subjected to a given thermal treatment (mixed with a suitable surfactant), was added during the constant angular coefficient section of the decreasing curve, it was observed that, after this addition, the signal continued to follow a linearly decreasing trend although with a lower slope than the linear section preceding sample addition (see Fig. 5). The rate of oxygen consumption by the yeast cells actually decreased owing to the presence of toxic substances formed during sample heating, the toxicity of which was linked to the variation in angular coefficient in the straight line section, so that an index of respiratory inhibition "ρ" was defined as the one's complement of the ratio between angular coefficients, before and after the addition of the oil. More precisely the index of inhibition of respiratory activity (ρ) is expressed as: $\%\rho = [1 - (a'/a)] \times 100$, where a' and a are the slopes of the respective sections C and B of the curve reported in Fig. 5.

2.4.7. Detailed performance of the respirometric test

The measurements were performed by allowing the biosensor to stabilize, under magnetic stirring, in the glass cell thermostatted at 25 °C containing a fixed electrolytic solution (15 mL), isotonic with the yeast cell plasma (section A in Fig. 5). The next step was to add a standard glucose solution (final concentration 0.1% w/v), and the variation of dissolved oxygen concentration caused by the increase in the yeast cell respiration process was recorded as a function of time (section B of Fig. 5).

The oil (500 μL), previously mixed with surfactant, 9 + 1 (v + v) (Tergosoft GC, a commercial emulsifier composed of PEG 7 – glyceryl cocoate) was then added; the emulsifier played a fundamental role and, without it, the oil, which is insoluble in water, would form a layer on top and prevent accurate measurement. After adding the oil sample, the variation in O_2 concentration continued for another three minutes (section C in Fig. 5). At the end of this period the measurement was completed and the initial system conditions were rapidly restored for the subsequent determination. By measuring the two slopes in sections C and B, respectively, of the curve recorded, the percent index of respiratory inhibition ($\rho\%$) was obtained.

2.5. Kinetic processing of data

2.5.1. "Model-fitting" kinetic method

The so-called "model-fitting" method (Gao, Chen, & Dollimore, 1993) was used in both the present and previous studies (Amati et al., 2008; Vecchio et al., 2008). A detailed description of this procedure was given in a previous paper (Campanella, Nuccilli, Tomassetti, & Vecchio, 2008). Nevertheless, the most suitable

kinetic models, as described by appropriate integral $g(\alpha)$ and differential $f(\alpha)$ model functions (where α is the degree of conversion), respectively reported in literature, have been based on the best linear fit of the experimental data to the following relationship (Gao et al., 1993):

$$g(\alpha) = \int_0^{\alpha} d\alpha/f(\alpha) = k_{iso} \cdot t \quad (1)$$

Once the best $g(\alpha)$ function had been selected, the specific rate constant k_{iso} values were obtained at each isothermal temperature for the selected model from the slopes of the corresponding "best-fitting" $g(\alpha)$ versus t regression line.

2.5.2. Kinetic processing data of fatty acid breakdown, obtained using TG–DTG analysis

Solid-state decomposition kinetics is usually described by the following basic equation:

$$d\alpha/dt = k(T) \cdot f(\alpha) \quad (2)$$

where α is the degree of reaction defined as $\alpha = (w_i - w_T)/(w_i - w_f)$ (where w_i and w_f are the initial and final mass loss, while w_T is the mass loss at temperature T), $f(\alpha)$ is the model function, which assumes different mathematical forms depending on the reaction mechanism (Gao et al., 1993) and $k(T)$ is the specific rate constant, whose temperature dependence is commonly described by the Arrhenius equation:

$$k(T) = A \cdot \exp(-E/RT) \quad (3)$$

where E is the activation energy, A is the pre-exponential factor, R the gas constant and T the absolute temperature. Moreover, taking into account that under non-isothermal conditions the heating rate is $\beta = dT/dt$, $d\alpha/dt = d\alpha/(dT/\beta)$, where t is the time; combining Eqs. (2) and (3), gives:

$$d\alpha/dT = A/\beta \cdot \exp(-E/RT) \cdot f(\alpha) \quad (4)$$

The proposed kinetic analysis, based on dynamic model-free methods using data obtained at different fixed heating rates, β, seems to be the most reliable approach. Due to the complexity of the decomposition patterns of the examined materials the kinetic study was carried out using the Kissinger equation (Kissinger, 1957; Vecchio et al., 2008):

$$\ln(\beta/T_m^2) = \ln(AR/E) + (-E/R) \cdot (10^3/T_m) \quad (5)$$

where T_m is the DTG peak temperature at a given β value, A the pre-exponential factor, E the activation energy and R the gas constant. This equation gives the single activation energy from the slope of Eq. (5) for each step involving mass loss.

A kinetic study of decomposition steps was also performed using the isoconversional method of Ozawa–Flynn–Wall (OFW) (Flynn & Wall, 1966; Ozawa, 1965), which is based on the integral form of Eq. (2) in accordance with the following isoconversional equation:

$$\ln(\beta) = \ln(AR/E_\alpha) - \ln g(\alpha) - 5.3305 - 1.052 \cdot (E_\alpha/R) \cdot (10^3/T_\alpha) \quad (6)$$

Once the TG data had been processed, the corresponding activation energy values were derived from the slope of Eq. (6) for each value of the extent of reaction α, if Doyle's approximation (Doyle, 1962): $\ln p(x) - 5.3305 - 1.052x$, where $x = E/RT$ and $(20 \leqslant x \leqslant 60)$ is valid over the entire range of α.

3. Results and discussion

The aim in the present investigation was above all to study in depth the kinetic rate constant of the processes taking place in PO and defenolized EVOO, when they are oxidized at 180 °C in an air stream. To this end trends of two parameters were recorded using biosensors: the free radical formation (FRF) and the respirometric inhibition index (IRI) related to the toxicity index. Two experimentally recorded trends are displayed in Figs. 6 and 7, obtained respectively for PO and dephenolized EVOO isothermally heated at 180 °C.

Two different kinetic methods for processing data derived from biosensor measurements exploited during the isothermal breakdown at 180 °C of peanut and dephenolized extra virgin olive oils were used. The first method is called "model-fitting" (Gao et al., 1993) and is usually applied to processes occurring in solids. The second method, denoted as "classical kinetics" (Amati et al., 2008; Tomassetti et al., 2011), is applied to processes taking place in solution. Both methods enable the most suitable mechanism to be selected, i.e. the one displaying the best linear fit.

In order to calculate the kinetic constant data the method denoted as "model-fitting" was applied first. This method was used to seek the "model function" representing the best equation for describing the process. It involved the selection from among the most suitable kinetic models described by appropriate mathematical functions of the one that shows the best (linear) fit with the experimental data. To this end, the mathematical expressions of the most common differential and integral model functions ($f(\alpha)$ and $g(\alpha)$, respectively) found in literature (Gao et al., 1993) were considered, since only the actual integral function $g(\alpha)$, which represents the process examined, depends linearly on time, according to Eq. (1).

The investigation was therefore focused mainly on determining the kinetic constant at 180 °C, for the dual purpose of obtaining a "robust" value for this important kinetic parameter and of seeking

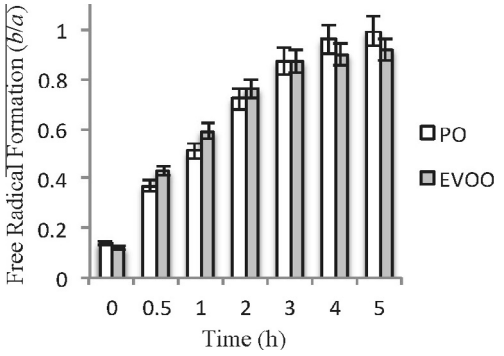

Fig. 6. Trends of the experimental b/a values (linked to free radical formation (FRF)) during the isothermal heating of peanut and dephenolized extra virgin olive oils (PO and EVOO, respectively) at 180 °C as a function of time.

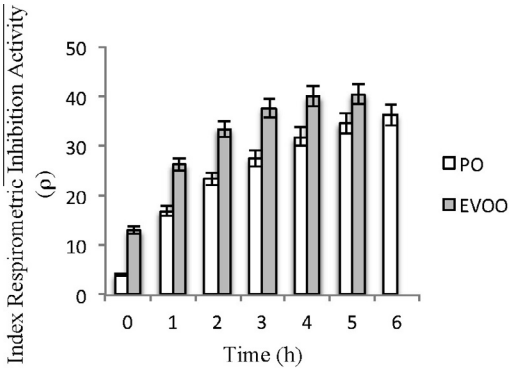

Fig. 7. Trends of the experimental values of the index of respirometric inhibition (IRI) during the isothermal heating of peanut and dephenolized extra virgin olive oils (PO and EVOO, respectively) at 180 °C as a function of time.

to establish which of the selected algorithms best fitted the above-mentioned processes. Once the best $g(\alpha)$ function was selected, the specific rate constant k_{iso} values at 180 °C were obtained from the slopes of the corresponding "best-fitting" $g(\alpha)$ versus t regression line, where $g(\alpha) = k_{iso}t$.

In previous studies (Amati et al., 2008; Campanella et al., 2008; Tomassetti et al., 2011), it was found that the best results may be obtained alternately using three possible algorithms that fit the decomposition processes considered. These algorithms are denoted as D1, F1 and F2, respectively:

$$D1: g(\alpha) = \alpha^2 \quad F1: g(\alpha) = -ln(1-\alpha) \quad F2: [1/(1-\alpha)] - 1 \tag{7}$$

Furthermore, in this study these three algorithms were therefore applied to decomposition process parameters of PO and dephenolized EVOO, recorded in the present research, i.e. the FRF and the IRI. To this end, the trends in the degree of conversion (α) of FRF and IRI for PO and EVOO are calculated as a function of time (see relative plots reported in Figs. 8 and 9). Then, the trends in the values of the integral function $g(\alpha)$ versus time t, for the best model functions selected (D1, F1 and F2) were evaluated (see Tables 1 and 2) and plotted in Figs. 10 and 11.

Lastly, Table 3 sets out the kinetic rate constant values found for peanut and dephenolized extra-virgin olive oils (PO and EVOO, respectively) during their thermal degradation occurring at 180 °C, as determined using the above illustrated isothermal model-fitting method, according to the trends of the index of the respirometric inhibition (IRI) and the b/a value linked to the free-radical formation index (FRF) for the three model function mechanisms selected (D1, F1 and F2).

Table 1
Values of the integral function $g(\alpha)$ for different working time t at 180 °C for the best model functions selected in order to monitor the free radical formation (FRF) for PO and EVOO.

Time (h)	Model function $g(\alpha)$					
	PO			EVOO		
	D1	F1	F2	D1	F1	F2
0	0.000	0.000	0.000	0.000	0.000	0.000
0.5	0.293	0.779	1.179	0.681	1.743	4.714
1	0.374	0.946	1.576	0.788	2.185	7.889
2	0.404	1.009	1.742	0.833	2.436	10.429
3	0.738	1.958	6.083	0.879	2.773	15.000
4	0.977	4.443	84.000	0.951	3.689	39.000
5	1.000			1.000		

Table 2
Values of the integral function $g(\alpha)$ for different working time t at 180 °C for the best model functions selected in order to monitor the index of respirometric inhibition (IRI) for PO and EVOO.

Time (h)	Model function $g(\alpha)$					
	PO			EVOO		
	D1	F1	F2	D1	F1	F2
0	0.000	0.000	0.000	0.000	0.000	0.000
1	0.158	0.507	0.660	0.762	2.061	6.857
2	0.359	0.915	1.496	0.826	2.398	10.000
3	0.533	1.309	2.701	0.894	2.909	17.333
4	0.627	1.570	3.806	0.964	4.007	54.000
5	0.839	2.479	10.926	1.000		
6	1.000					

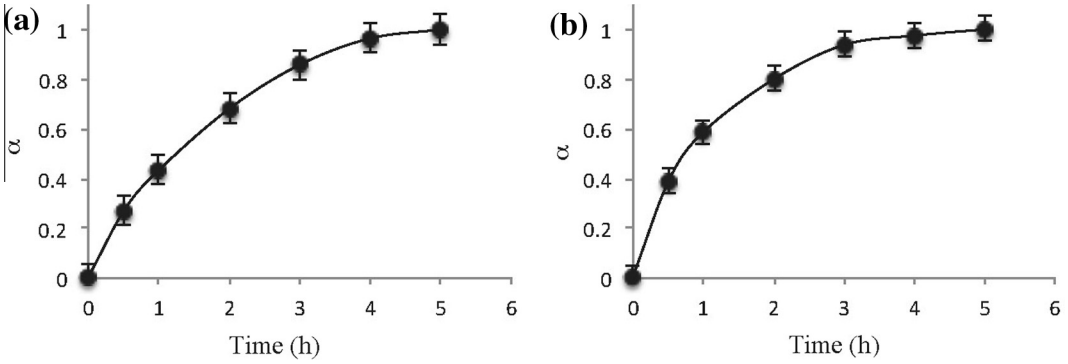

Fig. 8. Trends of the degree of conversion (α) values calculated using the b/a values (correlated with the free radical formation (FRF)) during the isothermal heating at 180 °C as a function of time for: (a) PO and (b) EVOO.

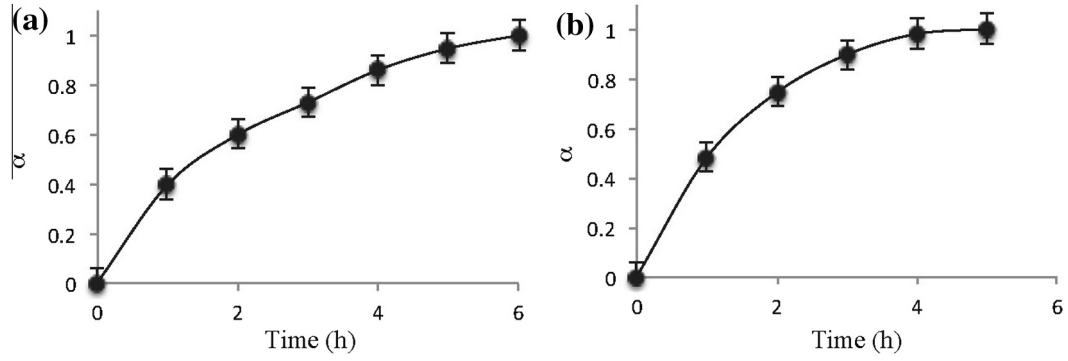

Fig. 9. Trends of the degree of conversion (α) values calculated using the Index of the Respirometric Inhibition (IRI) during the isothermal heating at 180 °C as a function of time for: (a) PO and (b) EVOO.

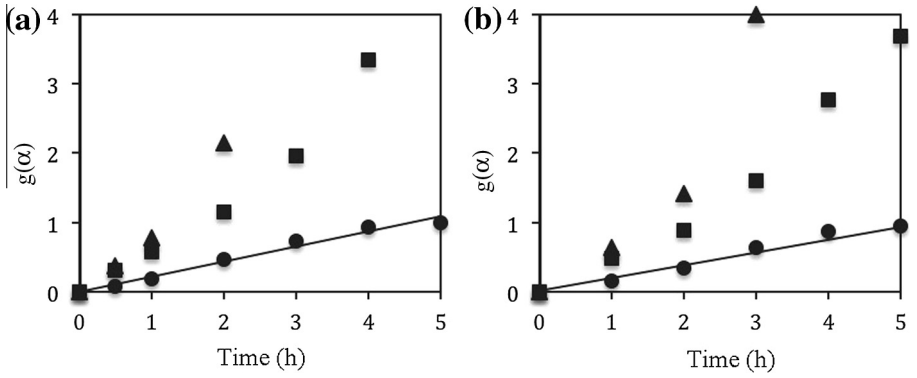

Fig. 10. Trends of the values of the integral function $g(\alpha)$ versus time t, for the best model functions selected (D1 (circles), F1 (squares) and F2 (triangles)) at the temperature considered (180 °C) in order to monitor the free radical formation (FRF) for (a) PO and (b) EVOO.

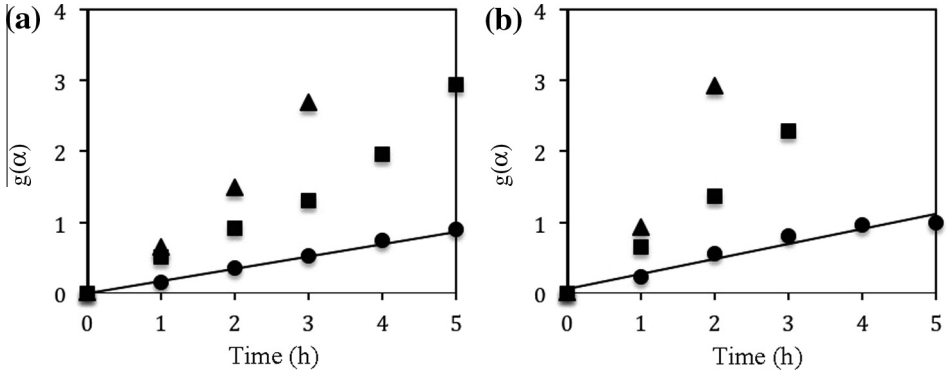

Fig. 11. Trends of the values of the integral function $g(\alpha)$ versus time t, for the best model functions selected (D1 (circles), F1 (squares) and F2 (triangles)) at the temperature considered (180 °C) in order to monitor the index of respirometric inhibition (IRI) for (a) PO and (b) EVOO.

Table 3
Kinetic rate constant found for peanut and dephenolized extra-virgin olive oils (PO and EVOO, respectively). Thermal degradation occurring at 180 °C as determined using the isothermal model-fitting method according to the trends of the index of the respirometric inhibition (IRI) and the b/a value correlated to the free-radical formation (FRF) for the three model function mechanisms selected (D1, F1 and F2).

Model function	10^{-3} k/min^{-1} (RSD ⩽ 4%)			
	From IRI index measurements		From FRF measurements	
	PO	EVOO	PO	EVOO
D1	3.1	3.5	4.1	4.1
F1	11.9	16.1	13.2	15.3
F2	51.1	193.1	96.3	148.3

Firstly, it should be noted that the k values thus obtained using two different indexes (IRI and FRF) are comparable, even though the units of IRI and FRF indexes used for the k computations are different. This is actually due to the fact that the variable used in the model functions considered (the degree of conversion α) is dimensionless. Secondly, judging not only and not so much on the basis of the goodness of the linear fit (e.g., the R^2 values), but also taking into account the strict uniformity (Amati et al., 2008; Tomassetti et al., 2011) of the k values obtained, D1 seems to be the model function which provides the most reliable results, at least in the operating conditions described above. Actually, the k values related to the thermal degradation of PO are not much different from those of dephenolized EVOO, which, when computed using the model function D1, are found to lie between (3.1 and 4.1) $\times$ 10^{-3} min^{-1}; actually, the k values obtained using the algorithm D1 applied to the processes (IRI) and (FRF) were always found to be of the order of 10^{-3} min^{-1} for both PO and EVOO. This value displays the same order of magnitude as that found also in a previous study (Amati et al., 2008) for the isothermal degradation of EVOO, working at the same temperature (180 °C), even though the processed trends in this case referred to parameters that differed from those investigated in the present work, that is, which had been obtained using other kind of biosensors to monitor the oil thermal degradation. In practice, regardless of the experimental parameter monitored, the values of the kinetic constants are found to be in all cases of the order of 10^{-3} min^{-1}, even if, of course, a certain variability of these values occurs according to the parameter considered.

Moreover, the k values found in the present research for the isothermal degradation of EVOO at 180 °C were, as expected, found to be significantly higher than those calculated for the oil breakdown process monitored at 98 °C reported in a previous study (Tomassetti et al., 2011) (see the values reported in Table 4). In this previous research the kinetic constant rate values of EVOO

Table 4
Kinetic constant rates of EVOO degradation occurring at 98 °C as determined respectively using the D1, F1 and F2 model functions derived from isothermal model-fitting method, according to the trends of thermal degradation of total polyphenols (TDTP), the total antioxidant capacity value (TACV), the peroxide number (PN), the hydroperoxide concentration (HP).

Model function	10^{-4} k/min^{-1} (RSD ⩽ 5%)			
	TDTP	TACV	PN	HP
D1	2.1	2.5	1.3	1.8
F1	3.6	8.9	0.6	1.1
F2	7.3	21.0	0.6	1.4

degradation occurring at 98 °C were determined respectively using the same D1, F1 and F2 model functions derived from the isothermal model-fitting method, but according to the trends of other different parameters (i.e. the thermal degradation of total polyphenols (TDTP), the total antioxidant capacity value (TACV), the peroxide number (PN) and the hydroperoxide concentration (HP) (Amati et al., 2008). Also in this case what has been determined so far is essentially the model function D1, which better describes the studied processes and the k values. The latter, calculated by model fitting for these processes, was found to be about one order of magnitude lower ($\approx 10^{-4}$ min^{-1}) than that obtained in the present research, in which the monitored parameters were on the contrary the free radical formation and the respirometric inhibition index and the thermo-oxidation of the PO and dephenolized EVOO oils was carried out a higher temperature, i.e.180 °C.

To obtain further information concerning the values found, for the latter parameter (k) and an estimation of the reaction order (n), which is also of considerable importance in order to complete the kinetic model, the values of the experimental curves in Figs. 6 and 7, referring to the two considered oil types and monitoring (IRI) and (FRF) during the oil degradation process, carried out at 180 °C under an air stream, were processed using classical kinetic methods, considering, according to the case, the reaction of zero, first, and second order, respectively, according to the well-known equations, briefly outlined below:

$$[A] = [A_0] - kt \quad \text{0 order reaction} \tag{8}$$

$$\ln[A] = \ln[A_0] - kt \quad \text{1st order reaction} \tag{9}$$

$$\frac{1}{[A]} = \frac{1}{[A_0]} + kt \quad \text{2nd order reaction} \tag{10}$$

where $[A]$ is the value of the parameter considered (IRI and FRF in this study) at time t and $[A_0]$ is the initial value at time zero.

The linear regression parameters found and the squares of the correlation coefficients of the three different kinetic equations applied referring to the degradation occurring at 180 °C in peanut oil (PO) and dephenolized extra-virgin olive oil (EVOO) are shown in Table 5, while in Table 6 the kinetic rate constant values, determined using the traditional kinetic method, according to the trends of the index of the respirometric inhibition (IRI) and the b/a value linked to the free-radical formation (FRF) for the three reaction orders selected are summarized and compared. Since all the R^2 values related to the three different reaction orders considered are found to be statistically equivalent, it is difficult to select the most suitable mechanism (and to establish an appropriate reaction order) on the basis of these values alone. However, it is worth noting that a very good agreement is found between the values of k obtained with the classical method using the first order reaction and those derived using the model-fitting method for the D1 model function.

Table 5
Linear regression parameters and square values of correlation coefficients of the three different kinetic equations applied related to the degradation occurring at 180 °C in peanut oil (PO) and dephenolized extra-virgin olive oil (EVOO).

Sample	IRI			FRF		
	Intercept (mol l^{-1})	$10^{-4}\cdot$ Slope[a]	R^2	Intercept (mol l^{-1})	$10^{-4}\cdot$ Slope[a]	R^2
0th order						
PO	9.91	836	0.7051	0.29	27	0.7063
EVOO	18.78	87	0.7459	0.34	24	0.6982
1st order						
PO	2.16	49	0.6954	−1.30	54	0.7291
EVOO	2.89	34	0.7463	−1.35	50	0.6940
2nd order						
PO	0.14	−4	0.4994	4.20	−140	0.5055
EVOO	0.06	−1	0.6418	4.43	−150	0.4065

[a] Units for slope values are mol l^{-1} min^{-1}, min^{-1} and mol^{-1} l min^{-1} for 0th, 1st and 2nd reaction orders, respectively.

Table 6
Rate constant values of thermal degradation of peanut and extravirgin olive oil (PO and EVOO, respectively) according to the classical kinetic method.

Reaction order (n)	10^{-3} k/min^{-1} (RSD ⩽ 7%)			
	From IRI index measurements		From FRF measurements	
	PO	EVOO	PO	EVOO
0	83.6	87.0	2.7	2.4
1	4.9	3.4	5.4	5.0
2	0.4	0.1	14.0	15.0

It should be also taken into account that the agreement of the values of k associated with the thermal degradation processes occurring in EVOO, olive oil (OO) and olive oil residue (OOR) at 98 °C, calculated in a previous study (Tomassetti et al., 2011) using the classical kinetic approach were also found to be quite good (for $n = 1$ reaction order), even if, of course, the k values were one order of magnitude lower (Tomassetti et al., 2011) than those at 180 °C.

It can reasonably be concluded that both the first reaction order ($n = 1$) and the model function D1 are the algorithms that best describe the processes investigated also in the present research, as well as in the previous study (Tomassetti et al., 2011).

On the other hand, in the present research, we also took into consideration the study of the thermal breakdown of the principal components of the PO oil matrix, namely the triglycerides, in an oxidizing atmosphere (air stream). In this case, the investigation was carried out using TG and DTG and processing the experimental TG/DTG data found for peanut oil recorded at four different heating rates by the Kissinger method (Kissinger, 1957). The thermal behaviour of peanut oil (PO) was analyzed by carrying out dynamic TG–DTG experiments at four different constant heating rates (2.5, 5.0, 8.0 and 12.5 °C min^{-1}) up to 550 °C (see Fig. 12).

The kinetic study is focused on the first two main processes, which occurred in the ranges 140–250 °C and 250–330 °C, respectively (Vecchio et al., 2008). Due to the complexity of the decomposition patterns referring to the samples examined, the kinetic study was carried out using Eq. (5), i.e. the Kissinger equation (Kissinger, 1957).

This equation gives a single activation energy from the slope of the straight line obtained for each main step involving mass loss (see the two straight lines obtained in Fig. 13 and the E and ln$A$ values obtained as reported in Table 7. Also in this case the kinetic data obtained were compared with those found in a previous study (Vecchio et al., 2008) in the same experimental conditions, but performed using whole extra virgin olive oil.

The kinetic study of the decomposition steps was also performed using the isoconversional method of Ozawa–Flynn–Wall (OFW) (Flynn & Wall, 1966; Ozawa, 1965), in accordance with Eq. (6). Once the TG data had been processed, the corresponding activation energy values were derived from the slope of the above-cited equation for each value of the extent of reaction α assuming that Doyle's approximation (Doyle, 1962) is valid over the entire range of α.

As can be seen from the TG/DTG curves in Fig. 12, two main thermal decomposition steps occur (from 140 and 330 °C) which are ascribable to the thermal breakdown of fatty acid chain residues of saturated and unsaturated triglycerides, respectively (Vecchio et al., 2008). Therefore, a deconvolution of the related DTG peaks (actually into three peaks) was performed in order to

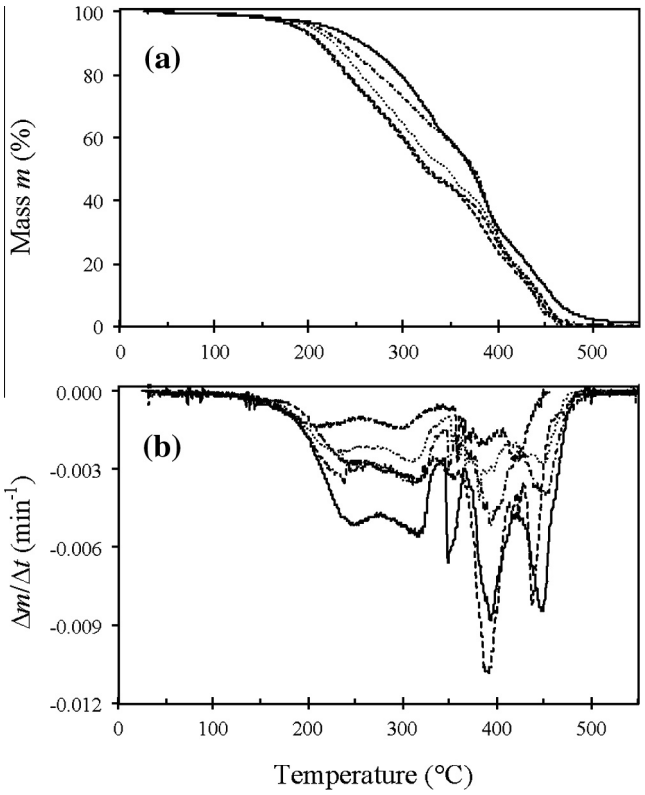

Fig. 12. TG (a) and DTG (b) curves of PO under the five heating rates considered between 2.5 and 12.5 K min^{-1}.

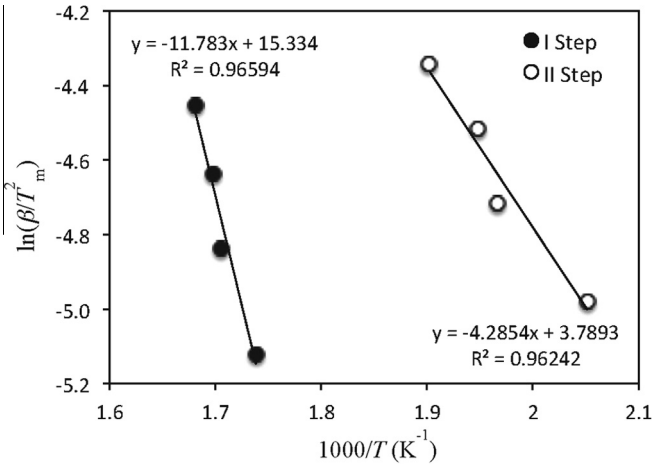

Fig. 13. Kissinger plot related to the two main decomposition steps of PO and the corresponding linear regression equations.

Table 7
Arrhenius parameters for the two main TG/DTG decomposition steps of triglycerides fatty acids contained in PO and EVOO.

Sample	First step (RSD ⩽ 8%)		Second step (RSD ⩽ 6%)	
	E (kJ mol^{-1})	ln(A/min^{-1})	E (kJ mol^{-1})	ln(A/min^{-1})
PO	35.6	12.2	98.0	24.7
EVOO[a]	78.0	15.0	156.0	30.1

[a] Values taken from Vecchio et al. (2008).

determine precisely the initial and final decomposition temperatures (T_i and T_f, respectively) of each process, as these are crucial data for obtaining reliable values of the degree of conversion α for each deconvoluted step.

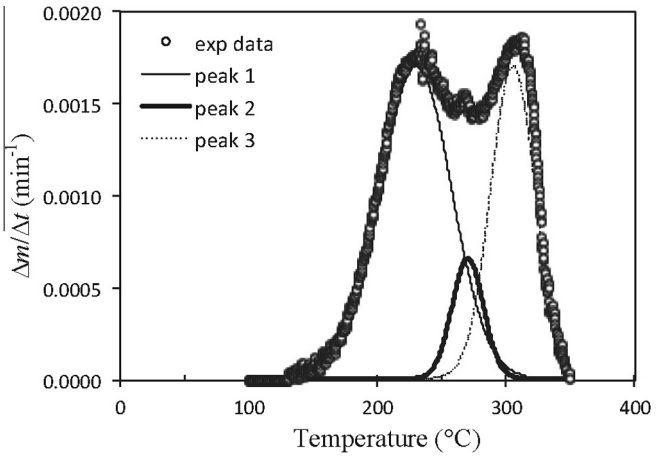

Fig. 14. Deconvolution of DTG peaks related to the overlapping triglyceride decomposition process of PO into three "Gaussian" peaks at a heating rate of 2.5 K min^{-1}.

The deconvolution of DTG peaks related to the overlapping thermal decomposition processes of PO into three "Gaussian" peaks at a heating rate of 2.5 °C min^{-1} is displayed in Fig. 14.

The initial and final temperatures for each of the two main deconvoluted peaks were used to define more precisely the beginning ($\alpha = 0$) and the end of each step ($\alpha = 1$).

The small DTG peak between two main DTG peaks, probably ascribable to the thermal degradation of very low percentages of glycerides other than triglycerides contained in the oil, was not further investigated. In Fig. 15 the conversion dependency of

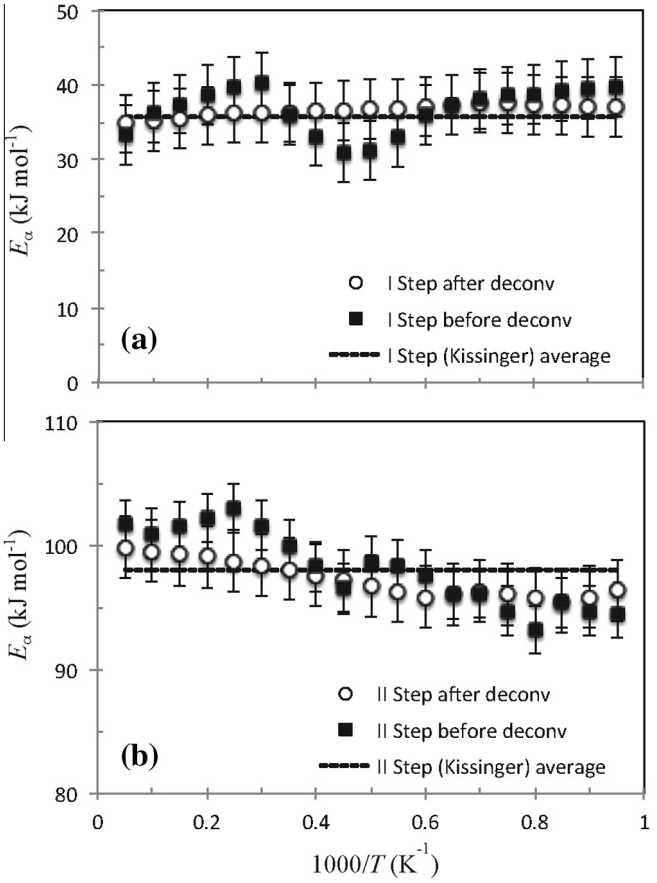

Fig. 15. Conversion dependency of E_α values related to the two main decomposition steps obtained using the isoconversional OFW method.

Table 8
Comparison of E data for the two main TG/DTG degradation processes of triglycerides' fatty acids found by Kissinger and OFW methods, or taken by literature for PO and whole EVOO.

	E /kJ mol^{-1}				
	Kissinger method		OFW method		Results taken from literature
	First step	Second step	First step	Second step	
PO	35.6	98.0	≈36–37	≈98	84.6–90.6[a]
EVOO	78.0	156.0	67.4–86.3	122.3–213.7	≈98[b]

[a] Kasprzycka-Guttman, Jarosz-Jarszewska, and Litwinienko (1995).
[b] Santos et al. (2004).

activation energy is shown for the thermal decomposition of both the two main processes examined. Note also how the deconvolution of DTG peaks gives more reliable activation energy values due to a more precise evaluation of the initial and final temperatures of each step. After deconvolution, the variation in activation energy values with α is quite negligible for each of the two steps, and the mean values of E found for the two main processes investigated are found to be equal to $E = 36.6$ and 98.2 kJ mol^{-1}, respectively.

Lastly, in Table 8, the E values obtained in the present research using the Kissinger method, OFW method and a few results drawn from the literature (in which it was not actually specified whether the values refer to the first or the second mass loss step) are compared. It is apparent how the values of E found for the isothermal breakdown of PO are slightly lower than those obtained previously for the same process occurring in whole EVOO; this is certainly due to the fact that in the latter case the EVOO was not dephenolized (Flynn & Wall, 1966). The presence of polyphenols therefore increases the activation energy of the thermo-oxidative process of EVOO, although the value of E remains approximately of the same order of magnitude.

4. Conclusions

With regard to the thermal-oxidative breakdown study of peanut oil at 180 °C and the comparison of results obtained for dephenolized extra-virgin olive oil undergoing the same process using two different methods based on very different approaches (model-fitting and classical kinetics) the algorithms corresponding to D1 and the first-order reaction were selected respectively as being experimentally indicated as the best.

From the slopes of the regression lines adopted in both methods the k kinetic rate constant values at 180 °C obtained for the isothermal breakdown of both peanut and dephenolized extra-virgin olive oils were of about 10^{-3} min^{-1}.

The k values, when referred to the EVOO breakdown at 180 °C, although monitored using other suitable parameters (Amati et al., 2008), are of the same order of magnitude as that found by processing two parameters monitored using two biosensor methods employed in the present study, and are, as expected, one order of magnitude higher than those calculated at 98 °C (Tomassetti et al., 2011).

Heating PO and dephenolized EVOO at 180 °C the average $t_{1/2}$, obtained from more reliable kinetic constant values found in the present research and for a first-order process is about 2.5 h. Therefore, the highest level of radical concentration and the highest toxicity level are reached after about 5 h. After this time radical level and toxicity remain more or less constant.

Lastly, the TG study of the thermal degradation of triglycerides contained in PO displayed lower E values than those related to the thermal degradation of triglycerides contained in whole EVOO found in previous research (Amati et al., 2008). This result cannot be explained on the basis of the glyceride composition since the main components in both oils are triglycerides, in particular glycerine trioleate (Kirk-Othmer, 1980; Nagy et al., 2005). Probably, this result is due to the extremely high concentration of polyphenols contained in the whole EVOO sample, while they are completely absent in PO.

It can be concluded that the reaction constant rates k of the processes related to both the free radical formation and the increasing toxicity index found in both PO and dephenolized EVOO heated at 180 °C do not seem to differ significantly. Conversely, the higher E values of the thermal degradation of whole EVOO, that is the higher thermal stability of triglycerides contained in the whole EVOO, is probably due to the high concentration of polyphenols contained in it.

Acknowledgement

This work was funded by "La Sapienza" University of Rome: University Project.

References

Amati, L., Campanella, L., Dragone, R., Nuccilli, A., Tomassetti, M., & Vecchio, S. (2008). New investigation of the isothermal oxidation of extra virgin olive oil: Determination of free radicals, total polyphenols, total antioxidant capacity, and kinetic data. *Journal of Agricultural and Food Chemistry, 56*, 8287–8295.
AOCS (1964). Methods Cd 12-57. In Official and tentative method of the American oil chemist's society (Vol. 1, 3rd ed., pp. 1-4). Champaign, IL: AOCS.
Biffoli, R. (1984). *Chimica degli Alimenti*. Firenze, Italy: USES.
Buzás, I., Simon, J., & Holló, J. (1979). Study of thermooxidative behaviour of edible oils by thermal analysis. *Journal of the American Oil Chemists Society, 56*, 685–688.
Campanella, L., De Luca, S., Favero, G., Persi, L., & Tomassetti, M. (2001a). Superoxide dismutase biosensors working in non-aqueous solvent. *Fresenius' Journal of Analytical Chemistry, 369*, 594–600.
Campanella, L., Dragone, R., Fisco, L., & Tomassetti, M. (2004). Study of toxicity and variation in polyphenol and hydroperoxide content of food oils subjected to thermal stress or used for frying foodstuffs. *Analytical Letters, 37*, 3047–3061.
Campanella, L., Favero, G., Pastorino, M., & Tomassetti, M. (1999). Monitoring the rancidification process in olive oils using a biosensor operating in organic solvents. *Biosensors and Bioelectronics, 14*, 179–186.
Campanella, L., Nuccilli, A., Tomassetti, M., & Vecchio, S. (2008). Biosensor analysis for the kinetic study of polyphenols deterioration during the forced thermal oxidation of extra-virgin olive oil. *Talanta, 74*, 1287–1298.
Campanella, L., Sammartino, M. P., Tomassetti, M., & Zannella, S. (2001b). Hydroperoxide determination by a catalase OPEE: Application to the study of extra virgin olive oil rancidification process. *Sensors and Actuators B, 76*, 158–165.
Carrasco-Pancorbo, A., Cerretani, L., Bendini, A., Segura-Cerretero, A., Lercker, A., & Fernandez-Gutierrez, A. (2007). Evaluation of the influence of thermal oxidation on the phenolic composition and on the antioxidant activity of extra-virgin olive oils. *Journal of Agricultural and Food Chemistry, 55*, 4771–4780.
Chiavaro, E., Vittadini, E., Rodriguez Estrada, M. T., Cerretani, L., Bonoli, M., Bendini, A., et al. (2007). Monovarietal extra virgin olive oils: Correlation between thermal properties and chemical composition. *Journal of Agricultural and Food Chemistry, 55*, 10779–10786.
Doyle, C. D. (1962). Estimating isothermal life from thermogravimetric data. *Journal of Applied Polymer Science, 6*, 639–642.
Flynn, J. H., & Wall, L. A. (1966). A quick, direct method for the determination of activation energy from thermogravimetric data. *Journal of Polymer Science Part B: Polymer Letters, 4*, 323–328.
Gao, X., Chen, D., & Dollimore, D. (1993). The correlation between the value of α at the maximum reaction rate and the reaction mechanisms: A theoretical study. *Thermochimica Acta, 223*, 75–82.
Kasprzycka-Guttman, T., Jarosz-Jarszewska, M., & Litwinienko, G. (1995). Specific heats and kinetic parameters of thermo-oxidative decomposition of peanut oil. *Thermochimica Acta, 250*(1), 197–205.
Kiritsakis, A., & Markakis, P. (1987). Advances in food research. In C. O. Chichester (Ed.), *Olive oil: A review* (pp. 453–482). Academy Press Inc.
Kirk-Othmer (1980). *Fats and Fatty Acids Encyclopedia of Chemical Technology* (3rd ed.). New york: Wiley. Vol. 9, 808pp.
Kissinger, H. E. (1957). Reaction kinetics in differential thermal analysis. *Analytical Chemistry, 29*, 1702–1706.
Kurtz, J. E., Dufour, P., Duclos, B., Bergerat, J. P., & Exinger, F. (2004). *Saccharomyces cerevisiae*: An efficient tool and model system for anticancer research. *Bulletin Cancer, 91*, 133–139.
Lorusso, S., & Zelinotti, T. (1985). Alcuni indici analitici per la valutazione del grado di alterazione di grassi sottoposti a riscaldamento. *La Rivista della Società Italiana dell'Alimentazione, 3*, 209–214.

Nagy, K., Bongiorno, D., Avellone, G., Agozzino, P., Ceraulo, L., & Vekey, J. (2005). High performance liquid chromatography–mass spectrometry based chemometric characterization of olive oils. *Journal Chromatography, 1078*, 90–97.

Ozawa, T. (1965). A new method of analyzing thermogravimetric data. *Bulletin of the Chemical Society of Japan, 38*, 1881–1882.

Santos, J. C. O., Santos, I. M. G., Conceiçao, M. M., Porto, S. L., Trindade, M. F. S., Souza, A. G., et al. (2004). Thermoanalytical, kinetic and rheological parameters of commercial edible vegetable oils. *Journal of Thermal Analysis and Calorimetry, 75*, 419–428.

Tan, C. P., & Che Man, Y. B. J. (2000). Differential scanning calorimetric analysis of edible oils: Comparison of thermal properties and chemical composition. *Journal of the American Oil Chemists' Society, 77*, 143–155.

Tomassetti, M., Vecchio, S., & Campanella, L. (2011). Biosensors and other more traditional methods for the development of kinetic models to describe the isothermal rancidification process in several kinds of olive oils. *Current Analytical Chemistry, 7*, 207–215.

Vazquez Roncero, A., Janer Del Valle, M. I., & Janer Del Valle, C. (1973). Determination of total phenols in olive oil. *Grasas y Aceites, 24*, 350–355.

Vecchio, S., Campanella, L., Nuccilli, A., & Tomassetti, M. (2008). Kinetic study of thermal breakdown of triglycerides contained in extra-virgin olive oil. *Journal of Thermal Analysis and Calorimetry, 91*, 51–56.

Vecchio, S., Cerretani, L., Bendini, A., & Chiavaro, E. (2009). Thermal decomposition study of monovarietal extra virgin olive oil by simultaneous TG/DSC: Relation with chemical composition. *Journal of Agricultural and Food Chemistry, 57*, 4793–4800.